

# GaN THIN FILM PHOTOCATHODES FOR HIGH BRIGHTNESS ELECTRON BEAMS

M. Vogel<sup>†</sup>, M. Schumacher, X. Jiang, Institute of Materials Engineering, University Siegen, 57076, Siegen, Germany

## Abstract

Gallium nitride (GaN) is one promising candidate as photocathode material showing high quantum efficiencies which is one of the requirements for high brightness electron beams. In addition to reported quantum efficiencies of up to 70 %, GaN needs to satisfy the demands for long lifetime, low dark current and low thermal emittance. In this contribution, the ongoing activities of the synthesis by means of reactive rf magnetron sputtering and characterization of GaN is presented. The latter is done by standard materials science methods and in-situ measurements of the quantum efficiency in combination with lifetime and dark current measurements to assess and optimize the photocathode's performance. Along with the project's details, first experimental results of GaN thin films synthesized utilizing a GaAs source are presented.

## INTRODUCTION

High brightness, cw-capable electron injectors are playing a key-role in modern light sources based on the principles of energy recovery linacs (ERL) and free electron lasers (FEL). To operate such electron injectors photocathodes offering a high quantum efficiency (QE), long lifetime, low thermal emittance, and low dark current are required [1-3]. In this contribution we investigate the feasibility of employing GaN as photocathode material. GaN is a semiconductor material with an intrinsic band gap of 3.44 eV, corresponding to a wavelength of 360 nm. This bandgap, however, can be tailored to lower energies i.e. higher wavelengths by adding In. Provided that the stoichiometric control of  $\text{In}_x\text{Ga}_{1-x}\text{N}$  is possible from GaN ( $x = 0$ ) to InN ( $x = 1$ ) this bandgap engineering leads to excitation wavelength between UV (3.4 eV) and infrared (0.8 eV) [4]. A reported QE of more than 70%, very low dark current and the chemical stability (stable in air) makes GaN a promising candidate as photocathode material [5].

To exploit GaN as photocathode material, it is necessary to alter its intrinsic properties to form a negative-electron-affinity (NEA) photoemitter. On the one hand, the semiconducting material must be heavily p doped so that the distance over which the valence- and conduction bands bend is short, and the Fermi level is near the top of the valence band. Mg is used as dopant with doping levels of up to  $10^{20} \text{ cm}^{-3}$ , although, there seems to be an optimum level around  $10^{17} \text{ cm}^{-3}$  in terms of maximum QE [6]. On the other hand, the work-function of the surface must be lowered in order to bring the energy level of the vacuum to the same or to a lower level than the energy level of the conduction-band minimum. This is achieved by coating the

GaN surface with a very thin film (some nm) of Cs or  $\text{Cs}_2\text{O}$ .

Given that in this work the semiconducting material is deposited directly onto the metal cathode body, we may suffer from a poor electric conductivity between coating and substrate due to the Schottky effect. The separation of charge, however, can be prevented by adding a 1-2 nm thick  $\text{TiO}_x$  interlayer between metal and semiconductor and, consequently, improving the conductivity [7]. Besides that, there might be the potential of improving the electron emission through a careful adjustment of the film thickness as well as the complex refractive indices of film and substrate [8]. Again, the latter can be achieved by a careful selection of an interlayer or a substitution of material of the metal cathode itself.

In this contribution we keep record on the ongoing construction of the experimental setup, give some details on the synthesis and characterization of the thin film system and report some preliminary experimental results.

We reported on some aspects of this project previously [9]. Here, a paper was cited describing a QE measurement of a GaN photocathode of up to 68.7 %. This paper, however, was retracted a few months after publication [10, 11] – we apologise for the confusion that this may have caused.

## EXPERIMENTAL

A schematic of the experimental setup is given in Figure 1. The sample flow starts from the load lock. After loading the sample onto the sample manipulator the load lock is evacuated and then transferred to the synthesis chamber. Here, samples can be cleaned utilizing an ion gun ( $\text{H}^+$ ,  $\text{He}^+$ ,  $\text{Ar}^+$  can be chosen) and coated. The latter is done by a sputter cluster, composed of four sputter cathodes 2" in diameter each. The cathodes are equipped with a shutter, gas injection and a chimney to minimize cross contamination of the targets. Contrary to the sketch, the cathodes are sitting on a circle, confocally arranged with their intersection point on the substrate. The Ga source is made from high purity GaN (6N), all other materials (In, Mg, Ti) are high purity metals (6N). Metallic Ga's melting point is at  $29.8^\circ\text{C}$  and therefore not suitable as normal sputter cathode. The sputtering takes place at different partial pressures of  $\text{N}_2$  and Ar (Ar :  $\text{N}_2$  flow from 0 to 1), variable substrate temperature (room temperature  $< T < 800^\circ\text{C}$ ), target power ( $40 \text{ W} < P < 300 \text{ W}$ , all four target powers set individually), and process pressure ( $0.2 < p < 2 \text{ Pa}$ ). At the time of publishing, this sputter cluster is going to be installed. Results shown here originated from a single 4" GaAs target driven up to 600 W of target power.

<sup>†</sup>michael.vogel@uni-siegen.de

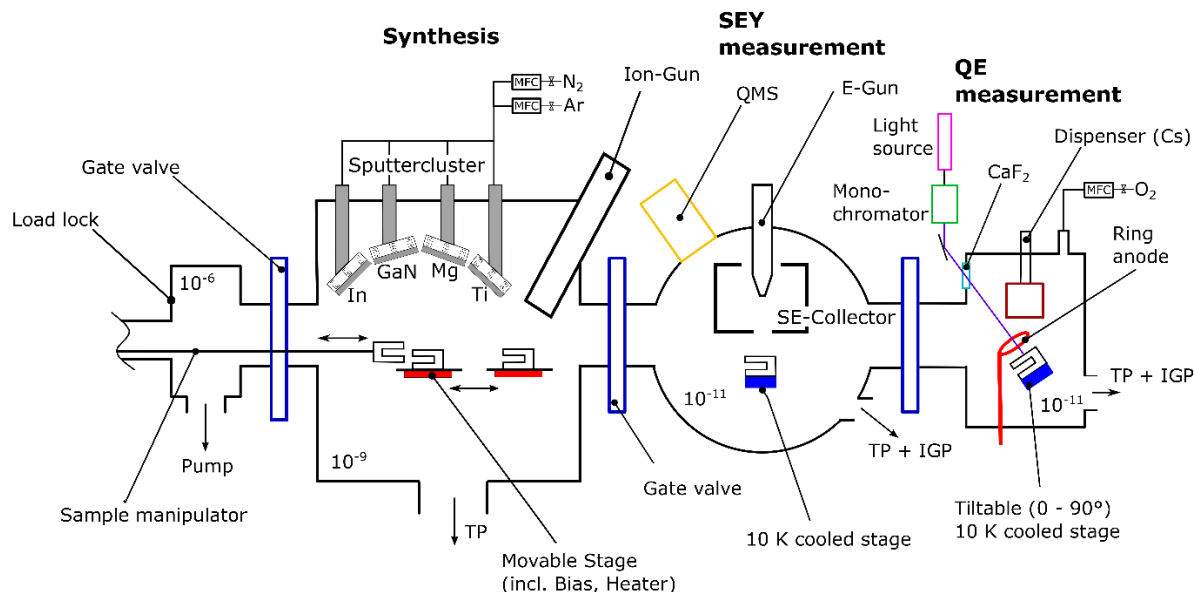


Figure 1: Experimental setup for the synthesis, cleaning and measurement of GaN samples.

After cleaning and/or deposition, the sample is transferred to the quantum efficiency (QE) measurement setup. There is an option to measure the sample's secondary electron yield (SEY) in the depicted sketch. This setup, however, is part of a different investigation [12]. In the QE setup, the sample sits on a sample stage which is tiltable from 0° to 90° angle of light incidence and can be cooled down to 10K via a cryostat. A more detailed scheme is shown in Figure 2. A ring anode, 20 mm away from the sample's surface is biased up to 1,000 V collecting the photoelectrons. The activation of the GaN photocathode (NEA photoemitter) is carried out by evaporating Cs and eventually adding O<sub>2</sub> while the sample is illuminated by UV light. After finding the maximum electron yield the activation process is ceased.

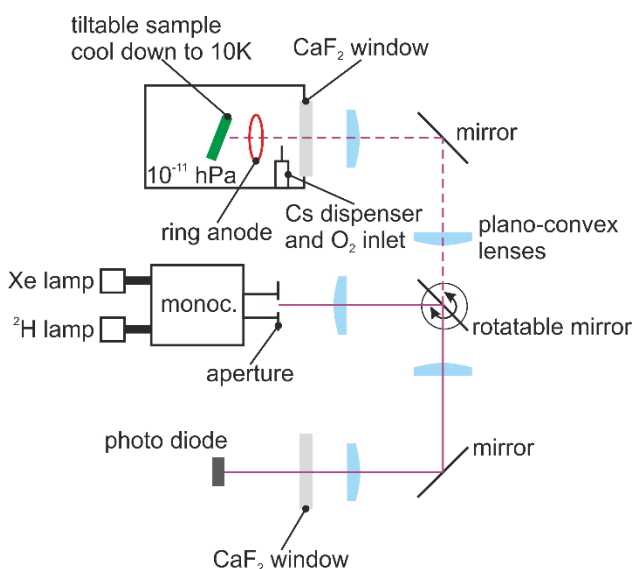


Figure 2: Detailed representation of the QE measurement setup.

Finally, the QE measurement is performed under monochromatic light irradiation. The wavelength is swiped from 250 nm up to 1,200 nm in steps of e.g. 10 nm. At each measuring point the rotatable mirror is switched to measure the spectral power by a photo diode. At the time of publishing, the QE setup is under commissioning and we summarize some of the figures of merit and give an error calculation for the upcoming measurements.

## RESULTS AND DISCUSSION

The synthesis of GaN on Si and Cu is feasible from a GaAs target. Besides structural characterization, the main finding is the depletion of As content inside the coatings by increasing the substrate temperature during deposition. However, even at deposition temperatures of 800°C the measured atomic content of As by means of EDX stays at around 1%. The impact of such a high As content on the QE and related properties will be investigated as soon as the in-situ measurement setup is ready. To avoid the contamination by As the formerly mentioned GaN target will be applied in the future experiments. SEM investigations shown in

Figure 3 reveal a fine columnar growth with column diameters of 10 to several tenth of nm.

The rms roughness measured by means of AFM is found to be pressure dependent. At the lower end of the process pressure (lower than 0.8 Pa) the roughness increases to 2.5 nm whereas the roughness at higher process pressures is around 1 nm or below. These values are measured on GaN coated Si wafers with a Si wafer rms roughness of 0.5 nm. Similar values are measured on mirror polished Cu substrates whereas the polishing process leads to a surface rms roughness of 1 nm and the GaN coatings have a minimum roughness of 6 nm.

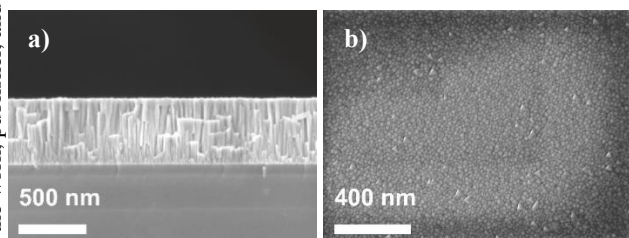


Figure 3: SEM micrographs of a) cross sectional and b) plain view GaN on Si.

The statistical roughness can be adjusted to higher values by wet chemical etching in a KOH solution. Figure 4 and Figure 5 show the resulting rms roughness at different etching times and etching temperatures, respectively. Changing the photoemitter's roughness to higher values leads to potentially higher QE values. Other characteristics like the dark current, however, may suffer from a high roughness. It is obvious that finding a compromise is key for the performance of the photocathode.

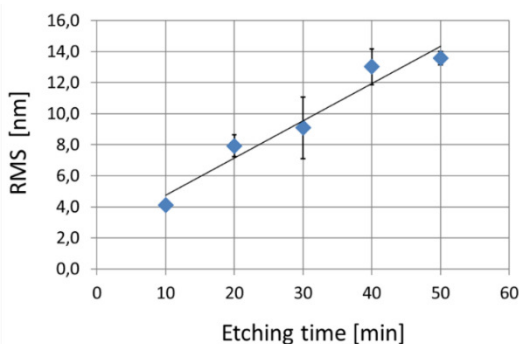


Figure 4: Rq over etching time in 1 molar KOH at 30 °C.

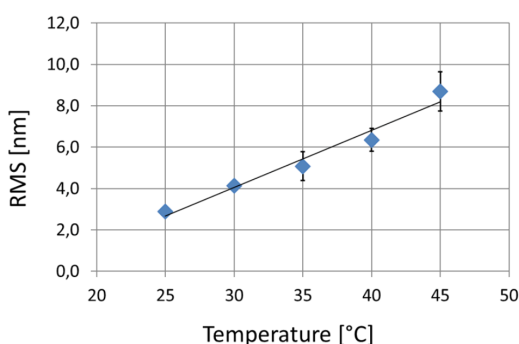


Figure 5: Rq over temperature in 1 molar KOH for 10 min.

Concluding, the commissioning of the ex-situ part of the QE setup is discussed. Figure 6 shows the drift of the Xe light source. It can be seen that after 45 minutes of warm up the lamp's output power is stable over time. An error analysis of all involved devices show a maximum error of 12 % in QE if the measurement is considered to be a single shot. Here the fluctuation in brightness shown as error bars in the diagram is the main error source. To mitigate these errors an integration of measurements lasting for 10 seconds reduces the error to 2 %, which is acceptable. If the

measurement is performed before the warm up is finished, the error rises to about 6.7 % again.

Another crucial parameter set of the optic setup is the slit width of the monochromator in- and output. Figure 7 and Figure 8 show the resulting maximum power output and bandwidth, respectively, as function of the slit width. One has to compromise between a reasonable power output and low enough band width. A slit width of 2 mm (both sides) leads to the workable bandwidth of 3.7 nm at 112  $\mu$ W.

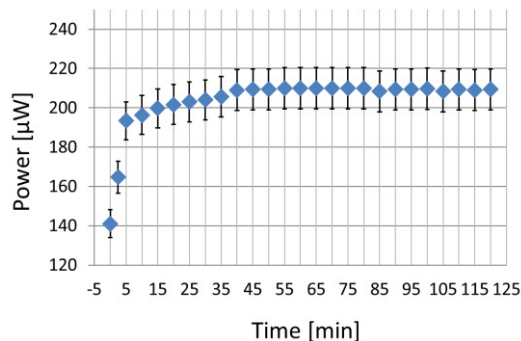


Figure 6: Drift of the Xe light source.

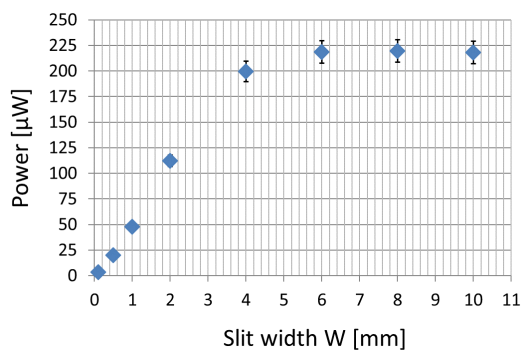


Figure 7: Light power at different slit width.

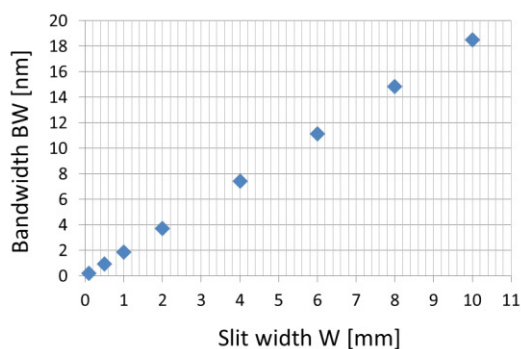


Figure 8: Resulting bandwidths at different slit widths.

## ACKNOWLEDGEMENT

This work was supported by the German Federal Ministry of Education and Research under grant 05K16PS1 "HOPE II: Hochbrillante photoinduzierte Hochfrequenz-Elektronenquellen".

## REFERENCES

- [1] M. Abo-Bakr, W. Anders, A. Büchel, K. Bürkmann-Gehrlein, P. Echevarria, A. Frahm, *et al.*, "Status of the Berlin Energy Recovery Linac Project BERLinPro," in *8th International Particle Accelerator Conference*, Copenhagen, Denmark, 2017, pp. 855-858.
- [2] A. Arnold and J. Teichert, "Overview on superconducting photoinjectors," *Physical Review Special Topics - Accelerators and Beams*, vol. 14, p. 024801, 02/02/ 2011.
- [3] B. Green, S. Kovalev, V. Asgekar, G. Geloni, U. Lehnert, T. Golz, *et al.*, "High-Field High-Repetition-Rate Sources for the Coherent THz Control of Matter," *Scientific Reports*, vol. 6, p. 22256, 02/29/online 2016.
- [4] J. Wu, W. Walukiewicz, K. M. Yu, J. W. A. III, E. E. Haller, H. Lu, *et al.*, "Small band gap bowing in In<sub>1-x</sub>Ga<sub>x</sub>N alloys," *Applied Physics Letters*, vol. 80, pp. 4741-4743, 2002.
- [5] S. Uchiyama, Y. Takagi, M. Niigaki, H. Kan, and H. Kondoh, "GaN-based photocathodes with extremely high quantum efficiency," *Applied Physics Letters*, vol. 86, p. 103511, 2005.
- [6] X. Wang, B. Chang, L. Ren, and P. Gao, "Influence of the p-type doping concentration on reflection-mode GaN photocathode," *Applied Physics Letters*, vol. 98, p. 082109, 2011.
- [7] P. J. King, E. Arac, S. Ganti, K. S. K. Kwa, N. Ponon, and A. G. O'Neill, "Improving metal/semiconductor conductivity using AlO<sub>x</sub> interlayers on n-type and p-type Si," *Applied Physics Letters*, vol. 105, p. 052101, 2014.
- [8] A. Alexander, N. A. Moody, and P. R. Bandaru, "Enhanced photocathode performance through optimization of film thickness and substrate," *Journal of Vacuum Science & Technology B, Nanotechnology and Microelectronics: Materials, Processing, Measurement, and Phenomena*, vol. 35, p. 022202, 2017.
- [9] M. Schumacher, M. Vogel, and X. Jiang, "GaN-based Photocathodes for High Brightness Electron Beams," in *18th International Conference on RF Superconductivity*, Lanzhou, China, 2017, pp. 906-909.
- [10] X. Guo, X. Wang, B. Chang, Y. Zhang, and P. Gao, "High quantum efficiency of depth grade doping negative-electron-affinity GaN photocathode," *Applied Physics Letters*, vol. 97, p. 063104, 2010.
- [11] X. Guo, X. Wang, B. Chang, Y. Zhang, and P. Gao, "Retraction: "High quantum efficiency of depth grade doping negative-electron-affinity GaN photocathode" [Appl. Phys. Lett. 97, 063104 (2010)]," *Applied Physics Letters*, vol. 98, p. 029901, 2011.
- [12] M. Vogel, C. Schlemper, and X. Jiang, "CARBON-BASED COATINGS FOR ELECTRON CLOUD MITIGATION IN SRF PHOTOCATHODES " in *18th International Conference on RF Superconductivity*, Lanzhou, China, 2017.